Letter

Out-of-time-order correlation as a witness for topological phase transitions

Qian Bin,[1] Liang-Liang Wan,[1] Franco Nori,[2,3,4] Ying Wu,[1] and Xin-You Lü[1,*]

[1]*School of Physics and Institute for Quantum Science and Engineering, Huazhong University of Science and Technology, Wuhan 430074, China*

[2]*Theoretical Quantum Physics Laboratory, RIKEN Cluster for Pioneering Research, Wako-shi, Saitama 351-0198, Japan*

[3]*RIKEN Center for Quantum Computing (RQC), 2-1 Hirosawa, Wako-shi, Saitama 351-0198, Japan*

[4]*Physics Department, The University of Michigan, Ann Arbor, Michigan 48109-1040, USA*

(Received 16 April 2022; accepted 20 January 2023; published 31 January 2023)

We propose a physical witness for dynamically detecting topological phase transitions (TPTs) via an experimentally observable out-of-time-order correlation (OTOC). The distinguishable OTOC dynamics appears in the topological trivial and nontrivial phases due to the topological locality. In the long-time limit, the OTOC undergoes a *zero-to-finite-value transition* at the critical point of the TPTs. This transition is robust to the choices of the initial state of the system and the operators used in the OTOC. The proposed OTOC witness can be applied to systems with and without chiral symmetry, e.g., the lattices described by the Su-Schrieffer-Heeger model, Creutz model, and Haldane model. Moreover, our proposal, as a physical witness in real space, is still valid even in the presence of disorder. Our work fundamentally brings the OTOC into the realm of TPTs and offers the prospect of exploring topological physics with quantum correlations.

DOI: 10.1103/PhysRevB.107.L020202

Topological phase transitions (TPTs) are fundamentally interesting in modern physics because these go beyond the paradigm of traditional phase transitions associated with symmetry breaking [1]. They offer a nontrivial paradigm for the classification of matter phases and thus are attracting enormous attention in condensed matter physics [2–5], optics [6], and non-Hermitian physics [7]. The occurrence of TPTs involves the gap closing and opening of bands (the change in system topology) with preservation of symmetry. According to the extended bulk-boundary correspondence, the nth-order TPT in a d-dimensional (dD) system leads to the appearance of a $(d-n)$-dimensional gapless boundary state in the topological nontrivial phase [8–19]. This symmetry-protected boundary state has strong robustness to disorder [20–22] and defects [23]. It can be used to realize topological lasers exhibiting robust transport [23–27], topological protected quantum coherence [28,29], and quantum state transfer [30]. Thus the detection of TPTs is a key for exploring topological physics. To quantitatively distinguish the topological trivial and nontrivial phases, normally one calculates topological invariants (e.g., winding number and Chern number) in momentum space [31]. However, identifying TPTs with those commonly used topological invariants is not suited for disordered systems, where it is difficult to give the Hamiltonian in momentum space. Then, it becomes a significant task to identify TPTs via an alternative physical witness in real space that is robust to disorder.

The out-of-time-order correlation (OTOC), defined as $\mathcal{O}(t)=\langle W^\dagger(t)V^\dagger W(t)V\rangle$ with $W(t)=e^{iHt}We^{-iHt}$, was proposed in investigating the holographic duality between a strongly interacting quantum system and a gravitational system [32–37]. Here, W and V are initially commuting operators [38]. Different from the normal time-order correlation function characterizing classical and quantum statistics [39–43], the OTOC can quantify the temporal and spatial correlations throughout many-body quantum systems, which are closely related to information scrambling. Thus it is a widely used tool for diagnosing chaotic behavior [44–62], many-body localization [63–70], entanglement [71–75], and quantum phase transitions [76–82]. Here, many-body localization is a kind of many-body phenomenon in the nonequilibrium system caused by many-body interactions. This is essentially different from TPTs that describe the change in the topological structure of systems. Under the framework of band topology theory, normally TPTs occur in the system without many-body interactions. Moreover, the OTOC can also be implemented experimentally [83–87] by connecting the time reversal to the Loschmidt echo technique [88–90]. Further exploiting OTOC dynamics in topological systems may open a door for completing the challenging problem of identifying TPTs in the presence of disorder. Until now, the relation between OTOC and TPTs remains largely unexplored, which may substantially advance the fields of quantum correlation and topological physics.

Here we propose an OTOC witness for dynamically detecting TPTs in lattice systems. As shown in Fig. 1(a), the constructed OTOC becomes an experimentally observable fidelity [83] of a final state ρ_f projected onto an initial state ρ_0 by defining $V=V\rho_0=|\psi_0\rangle\langle\psi_0|$, i.e.,

$$\mathcal{O}(t)=\mathrm{tr}[\rho_0 e^{iHt}W^\dagger e^{-iHt}\rho_0 e^{iHt}We^{-iHt}]=F(t). \quad (1)$$

Due to the topological locality, the long-time limit of the OTOC $\mathcal{O}(t\to\infty)$ undergoes a *zero-to-finite-value transition* along with the system entering into the nontrivial phase from the trivial phase. This sudden change is not limited by the choices of the operators V (corresponding to the initial state

*xinyoulu@hust.edu.cn

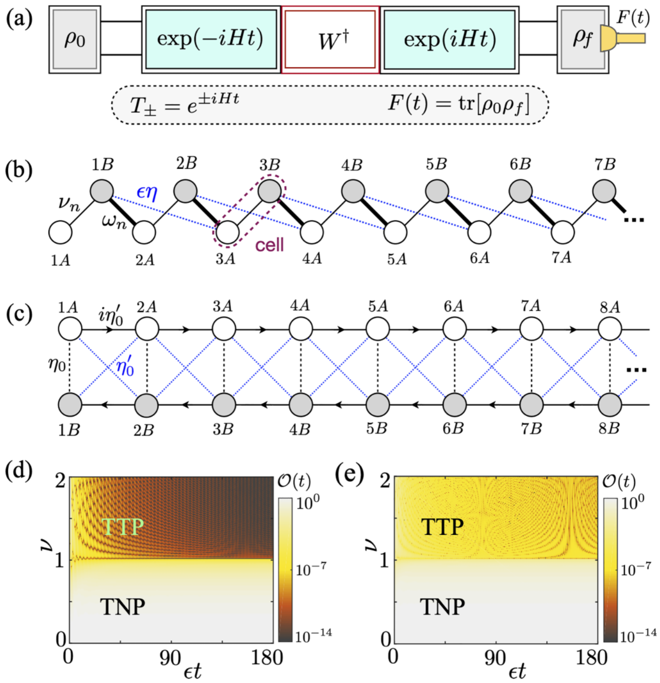

FIG. 1. (a) A schematic illustration of implementing the OTOC, which is equal to the fidelity $F(t) = \mathrm{tr}[\rho_0\rho_f]$ [73,83]. First, the initial state ρ_0 evolves into the state $\rho_1(t)$ under $T_- = e^{-iHt}$. Second, the system changes from $\rho_1(t)$ to $\rho_2(t)$ after the operation of W. Lastly, the system evolves backward to get the final state ρ_f under $T_+ = e^{iHt}$. (b) and (c) Schemes of the 1D SSH model and Creutz model, respectively, which describe lattice systems with chiral symmetry. (d) and (e) Phase diagrams of the NN SSH model: the OTOC vs ϵt and ν for $W = a_{1,A}^\dagger a_{1,A}$ (d) and $W = \sum_{n=1}^{N-1} a_n^\dagger\sigma_3 a_n$ (e), where $N = 200$, $|\psi_0\rangle = |1, A\rangle$ and $d_1 = d_2 = 0$. TNP and TTP, topological nontrivial and trivial phases, respectively.

of system) and W. In comparison with previous methods of detecting TPTs [5], the proposed OTOC, as a witness in real space, can be applied in *disordered systems*. Moreover, it not only is suitable for systems with chiral symmetry described by the nearest-neighbor (NN) Su-Schrieffer-Heeger (SSH) model, next-next-nearest-neighbor (NNNN) SSH model, and Creutz model, but also can be used for systems without chiral symmetry, such as two-dimensional (2D) lattices described by the Haldane model and Qi-Wu-Zhang model. We also demonstrate the validity of the OTOC witness for detecting second-order TPTs. Our work fundamentally broadens the realm of OTOC by bringing it to the next stage of application in topological physics.

Detecting TPTs in systems with chiral symmetry. Without loss of generality, we choose the 1D SSH model and Creutz model depicted in Figs. 1(b) and 1(c) as examples for demonstrating the validity of detecting TPTs with OTOC in systems with chiral symmetry. The corresponding system Hamiltonians can be written as [31,91–93]

$$H_\mathrm{S} = \sum_n \left\{ \nu_n a_n^\dagger \sigma_1 a_n + \left[(\omega_n a_{n+1}^\dagger + \epsilon\eta a_{n+2}^\dagger) \frac{\sigma_1 + i\sigma_2}{2} a_n + \mathrm{H.c.} \right] \right\}, \tag{2a}$$

$$H_\mathrm{Cr} = \sum_n \left\{ \eta_0 a_n^\dagger \sigma_1 a_n + \eta_0' \left[a_{n+1}^\dagger \frac{\sigma_1 - i\sigma_3}{2} a_n + \mathrm{H.c.} \right] \right\}, \tag{2b}$$

where the number of cells is N, σ_j $(j = 0, 1, 2, 3)$ is the Pauli operator, and $a_n^\dagger = (a_{n,A}^\dagger, a_{n,B}^\dagger)$ is the annihilation operator of the unit cell n with sublattices A and B. For the SSH model with Hamiltonian H_S, $\omega_n = \epsilon(1 + d_1 r_n)$ $[\nu_n = \epsilon(\nu + d_2 r_n')]$ is the intercell (intracell) hopping strength. Disorder with the dimensionless strengths d_1, d_2 has been included here, and r_n, r_n' are the independent random real numbers chosen from the uniform distribution $[-0.5, 0.5]$. Physically, ϵ is the characteristic intercell strength, ν is the ratio of intra- to intercell hopping in the clean system, and $\epsilon\eta$ is the NNNN hopping strength. Here, H_s is reduced to a standard Hamiltonian of the NN SSH model when $\eta = 0$. For the Creutz model with Hamiltonian H_Cr, the arrows in Fig. 1(c) indicate the sign of the hopping phase, and η_0 (η_0') is the vertical (horizontal and diagonal) hopping strength. The above models possess a chiral symmetry with a well-defined chiral operator $\mathcal{C}_\mathrm{1D}$, which can reverse the energy of the system, i.e., $\mathcal{C}_\mathrm{1D} H \mathcal{C}_\mathrm{1D}^{-1} = -H$ $(H = H_\mathrm{S}, H_\mathrm{Cr})$, where $\mathcal{C}_\mathrm{1D} = \sum_{n=1}^N a_n^\dagger \sigma_3 a_n$ for the SSH model and $\mathcal{C}_\mathrm{1D} = \sum_{n=1}^N a_n^\dagger \sigma_2 a_n$ for the Creutz model.

Let us first consider the case of no disorder, i.e., $d_1 = d_2 = 0$; the NN (NNNN) SSH model and Creutz model feature the TPTs at $\nu = 1$ $(\eta = 0, 1)$ and $\eta_0 = \eta_0'$, respectively [31,91–93]. To identify the topological nontrivial and trivial phases in real space, in Fig. 2, we numerically calculate the OTOC dynamics with Eq. (1), which involves backward evolution. Note that Fig. 2 includes the results for choosing different OTOC operators V and W. It clearly shows that both for the SSH model and for the Creutz model, the distinguishable OTOC dynamics appears in the nontrivial and trivial phases. Specifically, the OTOC evolves to a finite value and almost zero in the topological nontrivial and trivial phases, respectively [see the insets of Figs. 2(b), 2(d), and 2(f)]. This relates to the physical mechanism that the information does scramble in the trivial phase, while this scrambling is suppressed immensely in the nontrivial phase. There exists a *zero-to-finite-value transition* in the long-time limit of the OTOC, when the system enters into the nontrivial phase from the trivial phase. This distinguishable OTOC dynamics is robust to the initial state of the system (i.e., the operator V), which could be a single-site occupation or a multisite occupation state. Moreover, the averaged OTOC becomes discrete at the critical point, when the initial state is the eigenstate of the system whose eigenvalue has the lowest absolute value [94]. Figure 2 also shows that the OTOC witness is not limited by the choice of the operator W. In our proposal, the operator W can be either a few-site (including single-site) operation on sublattice A (e.g., $W = \sum_{l=1}^L a_{l,A}^\dagger a_{l,A}$, $L = 1, 2, 3$) or a multisite operation on sublattices A and B (e.g., $W = \sum_{n=1}^{N-1} a_n^\dagger \sigma_j a_n$, $j = 2, 3$), and the chosen operators W neither commute nor anticommute with the system Hamiltonian, i.e., $[W, H]_\pm \neq 0$.

To fully show the dependence of the OTOC witness on system parameters, we also calculate the analytical solution of $\mathcal{O}(t)$ under the condition of $N \gg 1$. Let us consider the NN SSH model as an example and choose $|\psi_0\rangle = \sum_{m=1}^M \frac{(-1)^{m-1}}{\sqrt{M}} |m, A\rangle$, where $M = 1$ corresponds to the case of a single-site occupation state, i.e., $|\psi_0\rangle = |1, A\rangle$. Here, m and A/B in state $|m, A/B\rangle$ represent the mth cell and sublattice A or B, respectively. Corresponding to $W = \sum_{l=1}^L a_{l,A}^\dagger a_{l,A}$ and

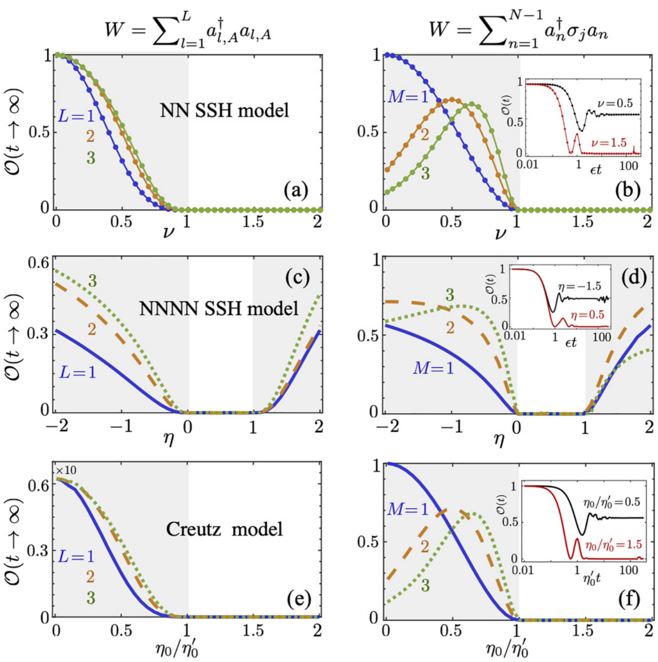

FIG. 2. The dependence of $\mathcal{O}(t\to\infty)$ on ν, η, and η_0/η_0' for (a), (c), and (e) $W=\sum_{l=1}^{L}a_{l,A}^{\dagger}a_{l,A}$ and (b), (d), and (f) $W=\sum_{n=1}^{N-1}a_n^{\dagger}\sigma_j a_n$ [$j=3$ for (b) and (d) and $j=2$ for (f)]. Results are for the systems described by the NN SSH model [(a) and (b)], NNNN SSH model [(c) and d)], and Creutz model [(e) and (f)]. The initial states are set as $|\psi_0\rangle=|1,A\rangle$ [(a), (c), and (e)], $|\psi_0\rangle=\sum_{m=1}^{M}(-1)^{m-1}|m,A\rangle/\sqrt{M}$ [(b) and (d)], and $|\psi_0\rangle=\sum_{m=1}^{M}(-1)^{m-1}(|m,A\rangle+i|m,B\rangle)/\sqrt{2M}$ (f). Insets in (b), (d), and (f): the evolution of the OTOC for different values of ν, η, and η_0/η_0' when $M=1$. The curves and dots correspond to the fully numerical simulations obtained by Eq. (1) and the analytical results obtained by Eqs. (3) and (4), respectively. Other system parameters are $N=200$, $d_1=d_2=0$, $\eta=0$ [(a) and (b)], $\nu=1$ [(c) and (d)]. The TNPs and TTPs are indicated by the shaded and unshaded areas, respectively.

$W=\sum_{n=1}^{N-1}a_n^{\dagger}\sigma_3 a_n$, we obtain [94]

$$\mathcal{O}(t)\approx\left[1/\sum_{n=0}^{N}\nu^{2n}+\sum_{k=1}^{N}\frac{2\epsilon^2\nu^2\cos(\lambda_{+}^{(k)}t)}{(N+1)(\lambda_{\pm}^{(k)})^2}\sin^2\left(\frac{k\pi}{N+1}\right)\right]^4 \tag{3}$$

and

$$\mathcal{O}(t)\approx\left[1/\sum_{n=0}^{N}\nu^{2n}+\sum_{k=1}^{N}\frac{2\epsilon^2\nu^2\cos(2\lambda_{+}^{(k)}t)}{(N+1)(\lambda_{\pm}^{(k)})^2}\sin^2\left(\frac{k\pi}{N+1}\right)\right]^2, \tag{4}$$

respectively, for $L,M=1$. Here, $\lambda_{\pm}^{(k)}=\pm\epsilon[1+\nu^2+2\nu\cos(\frac{k\pi}{N+1})]^{1/2}$ and $k=1,2,\dots,N$. Note that the above equations require $\nu\neq0$, and $\nu=0$ means that intracell hopping cannot occur, corresponding to $\mathcal{O}(t)=1$. The similar analytical results for $L,M>1$ are shown in the Supplemental Material [94]. As shown in Figs. 1(a) and 1(b), the analytical solutions also present a *zero-to-finite-value transition* of OTOC at the critical point of TPTs. This conclusion is valid for both the case of choosing W as a single-site operation and the case of choosing W as a multisite operation. Figures 2(a) and 2(b) show a very good agreement between the analytical solutions and the fully numerical simulations, which demonstrates the validity of our solutions.

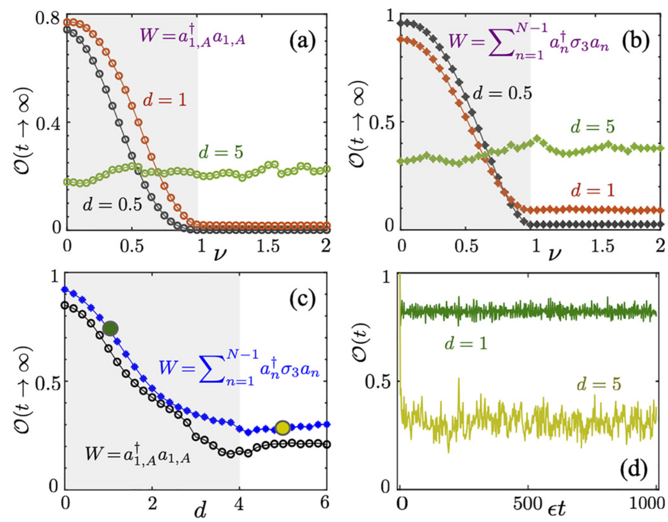

FIG. 3. (a) and (b) The dependence of $\mathcal{O}(t\to\infty)$ on ν for different disorder strengths d when (a) $W=a_{1,A}^{\dagger}a_{1,A}$ and (b) $W=\sum_{n=1}^{N-1}a_n^{\dagger}\sigma_3 a_n$. (c) The value of $\mathcal{O}(t\to\infty)$ vs d for different choices of the operator W when $\nu=0.2$. (d) The evolution of the OTOC for different d indicated by the large circles in (c). Here all data are averaged over 30 independent disorder configurations, and we have chosen $N=200$, $d_2=2d_1=d$, and $|\psi_0\rangle=|1,A\rangle$. The TNPs and TTPs are indicated by the shaded and unshaded areas, respectively.

Now let us discuss the influence of disorder on our proposal by choosing the NN SSH model as an example. The proposed OTOC witness for identifying the TPTs is also suitable for *disordered systems*. As shown in Figs. 3(a) and 3(b), $\mathcal{O}(t\to\infty)$ still undergoes the *zero-to-finite-value transition* along with the occurrence of the TPTs, even when weak disorder is introduced into the system. In terms of information, this transition originally comes from the topological locality in the nontrivial phase. Specifically, the information scrambling occurs in the trivial phase and is suppressed immensely in the nontrivial phase. Similarly to the case of no disorder, this result is robust to the choices of the operator W. Figures 3(a) and 3(b) also show that the above distinguishability of the OTOC dynamics disappears in the strong-disorder regime (e.g., $d>4$). Physically, this is because the TPTs, together with the symmetry-protected boundary state, will disappear as the disorder is too large. Figures 3(c) and 3(d) further demonstrate the vanishing of the topological nontrivial phase induced by strong disorder. Moreover, the proposed OTOC witness can also be considered as an order parameter of the topological phase diagram and predict topological Anderson insulator physics [94]. It is consistent with previous works in Refs. [20,22], which further verify the validity of our OTOC witness.

Detecting TPTs in systems without chiral symmetry. The proposed OTOC witness for identifying TPTs is not limited to the above systems with chiral symmetry, but is applicable for systems without chiral symmetry, such as 2D lattice systems described by the Haldane model and Qi-Wu-Zhang model.

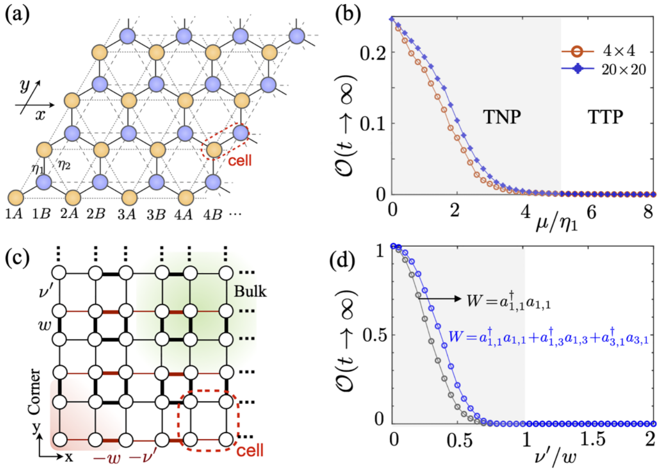

FIG. 4. (a) Scheme of the Haldane model, where the unit cell consists of sublattices A and B. (b) The dependence of $\mathcal{O}(t \to \infty)$ on μ/η_1 for different cell numbers when $|\psi_0\rangle = |1, A\rangle$ and $W = \sum_j c_j^\dagger c_j$ (the summation index j only covers all sublattice B sites). Here we have chosen $\eta_1 = \eta_2$ and $\phi = \pi/2$. The red and blue curves correspond to cell numbers of 4×4 and 20×20, respectively. (c) Scheme of the 2D SSH model with gauge flux π penetrating any plaquette. (d) The dependence of $\mathcal{O}(t \to \infty)$ on ν'/w for $W = a_{1,1}^\dagger a_{1,1}$ (black curve) and $W = a_{1,1}^\dagger a_{1,1} + a_{1,3}^\dagger a_{1,3} + a_{3,1}^\dagger a_{3,1}$ (blue curve) when $|\psi_0\rangle = |1, 1\rangle$. The TNPs and TTPs are indicated by the shaded and unshaded areas, respectively.

As shown in Fig. 4(a), the Haldane model on the honeycomb lattice has the Hamiltonian [106,107]

$$H_{\mathrm{Ha}} = \eta_1 \sum_{\langle j,j'\rangle} c_j^\dagger c_{j'} + \eta_2 \sum_{\langle\langle j,j'\rangle\rangle} e^{i s_{jj'}\phi} c_j^\dagger c_{j'} + \mu s' \sum_j c_j^\dagger c_j, \quad (5)$$

where $c_j^\dagger$ (c_j) is the creation (annihilation) operator of the jth site and the summation indices cover all sites. The symbol μ in the last term denotes the sublattice potential, where $s' = +1$ and $s' = -1$ correspond to sublattices A and B, respectively. Here, η_1 and η_2 are the real-valued nearest- and next-nearest-neighbor hopping amplitudes, respectively. The next-nearest-neighbor hopping contains the phases $s_{jj'}\phi$ with $s_{jj'} = \pm 1$, which can break the time-reversal symmetry. The system has no chiral symmetry and is a paradigmatic example of a 2D lattice featuring TPTs. For example, the parameter ranges $|\mu/\eta_2| < 3\sqrt{3}$ and $\mu/\eta_2 =$ other correspond to the topological nontrivial and trivial phases, respectively, when $\phi = \pi/2$. Using a procedure similar to the one used in 1D systems with chiral symmetry, we numerically calculate the OTOC dynamics with Eq. (1) to identify the occurrence of TPTs in real space. As shown in Fig. 4(b), the *zero-to-finite-value transition* of $\mathcal{O}(t \to \infty)$ can still be observed when the system enters into the topological nontrivial phase from the trivial phase. Similar results can also be obtained in the system described by the Qi-Wu-Zhang model [94].

Application to second-order TPTs. Higher-order topological insulators, as an extension of the topological insulators, have recently attracted extensive attention [8–19]. High-order TPTs usually can be identified by detecting the boundary states in real space. For example, topological protected corner states have been used to identify second-order TPTs in a 2D system [108–111]. Here, our proposed OTOC witness is also applicable for detecting second-order TPTs. As shown in Fig. 4(c), we take the extended 2D SSH model with nonzero gauge flux as an example, and its Hamiltonian reads [111]

$$\begin{aligned} H_{2\mathrm{S}}(\mathbf{k}) = {} & (\nu' + w\cos k_y)\tau_0 \otimes \sigma_1 - w \sin k_y \tau_3 \otimes \sigma_2 \\ & - (\nu' + w\cos k_x)\tau_2 \otimes \sigma_2 - w \sin k_x \tau_1 \otimes \sigma_2, \end{aligned} \quad (6)$$

where $\mathbf{k} = \{k_x, k_y\}$ is the wave number and $\pm\nu'$ ($\pm w$) is the intracell (intercell) hopping strength. This system features a second-order TPT when increasing the value of ν'/w, i.e., $\nu' < w$ and $\nu' > w$ corresponding to the topological nontrivial and trivial phases, respectively. To identify the occurrence of second-order TPTs, in Fig. 4(d), we numerically calculate the OTOC in the lattice system with 20×20 cells when the different OTOC operators W are considered. Figure 4(d) clearly shows the distinguishable OTOC dynamics in the topological nontrivial and trivial phases. Both for $W = a_{1,1}^\dagger a_{1,1}$ and for $W = a_{1,1}^\dagger a_{1,1} + a_{1,3}^\dagger a_{1,3} + a_{3,1}^\dagger a_{3,1}$, the *zero-to-finite-value transition* of $\mathcal{O}(t \to \infty)$ appears at the critical point of the second-order TPT. Moreover, the system is initially in the corner site (1,1) (i.e., $|\psi_0\rangle = |1, 1\rangle$), which is experimentally feasible. Here, (x, y) represents a lattice point in the square lattice, and $|x, y\rangle$ denotes the state occupying the site (x, y). The creation (annihilation) operator of the site (x, y) is denoted by $a_{x,y}^\dagger$ ($a_{x,y}$).

Experimental implementation and conclusions. Regarding experimental implementations, the trapped ion [83,112–115] is an ideal candidate for our proposal. We consider a set of $2N$ trapped ions with excited and ground states arranged along a 1D chain as the SSH model. First, the system is initialized in $\rho_0 = |1, A\rangle\langle 1, A|$ by applying a π pulse to excite the first ion in the chain into its excited state [113–115]. Then, one should make the system evolve under the Hamiltonian for a time t to the state $\rho_1(t) = e^{-iHt}\rho_0 e^{iHt}$. Subsequently, one applies the operator W to get $\rho_2(t) = W^\dagger \rho_1(t) W$. When the operator W is a single-site operator on sublattice A, this can be achieved by removing the polarizations of the ions except for that of the first ions by using selective pulses [83,113–115]. Next, the sign of H is inverted by the spin echo technique (i.e., applying a π pulse to reverse the polarization of one of the ions) [88], and the system is made to evolve again for t to obtain the final state, $\rho_f = e^{iHt}\rho_2(t)e^{-iHt}$ [89,90]. Finally, the OTOC can be obtained by measuring the overlap of the final state with respect to the initial state via fluorescence detection [83,115], similar to the many-body Loschmidt echo technique. For 2D lattice systems, the OTOC measurement is similar to that of the 1D lattice systems except for the construction of the model. Note that our proposal is not limited to this particular architecture and could be implemented or adapted on a variety of platforms that have full local quantum control [84–86,116–121], such as a nuclear magnetic resonance quantum simulator [84–86] and superconducting qubit [116–118].

In conclusion, we have proposed an OTOC witness in real space for identifying TPTs in general lattice systems with or without chiral symmetry. Our proposal is robust to the choices of the initial state of the system and the operators used in OTOC. It is also suitable for *disordered systems* and can predict topological Anderson insulator physics in the strong-disorder regime. Moreover, the proposed OTOC witness can be used to detect not only first-order TPTs, but also second-order TPTs. Applying it to non-Hermitian systems [94], the TPTs can be identified without implementing the transition from non-Bloch to Bloch theory. The generality of our proposal leads to the proposed OTOC witness having predictive power in detecting TPTs. For example, we could construct the OTOC witness by preparing the system initially in the first site and choosing a single-site operation as the W operator, even in a situation where we do not already understand the structure of a 1D lattice.

Acknowledgments. We thank Prof. T. Liu and Prof. J.-H. Gao for helpful discussions. This work is supported by the National Key Research and Development Program of China (Grant No. 2021YFA1400700), the National Natural Science Foundation of China (Grants No. 11974125, No. 12205109, and No. 12147143), and the China Postdoctoral Science Foundation (Grant No. 2021M701323). F.N. is supported in part by Nippon Telegraph and Telephone Corporation (NTT) Research, the Japan Science and Technology Agency (JST) [via the Quantum Leap Flagship Program (Q-LEAP) and Moonshot R&D Grant No. JPMJMS2061], the Japan Society for the Promotion of Science (JSPS) [via the Grants-in-Aid for Scientific Research (KAKENHI), Grant No. JP20H00134], the Army Research Office (ARO) (Grant No. W911NF-18-1-0358), the Asian Office of Aerospace Research and Development (AOARD) (via Grant No. FA2386-20-1-4069), and the Foundational Questions Institute Fund (FQXi) via Grant No. FQXi-IAF19-06.

[1] A. Bansil, H. Lin, and T. Das, Colloquium: Topological band theory, Rev. Mod. Phys. **88**, 021004 (2016).

[2] M. Z. Hasan and C. L. Kane, Colloquium: Topological insulators, Rev. Mod. Phys. **82**, 3045 (2010).

[3] X.-L. Qi and S.-C. Zhang, Topological insulators and superconductors, Rev. Mod. Phys. **83**, 1057 (2011).

[4] B. A. Bernevig and T. L. Hughes, *Topological Insulators and Topological Superconductors* (Princeton University Press, Princeton, NJ, 2013).

[5] C. K. Chiu, J. C. Y. Teo, A. P. Schnyder, and S. Ryu, Classification of topological quantum matter with symmetries, Rev. Mod. Phys. **88**, 035005 (2016).

[6] T. Ozawa, H. M. Price, A. Amo, N. Goldman, M. Hafezi, L. Lu, M. C. Rechtsman, D. Schuster, J. Simon, O. Zilberberg, and I. Carusotto, Topological photonics, Rev. Mod. Phys. **91**, 015006 (2019).

[7] E. J. Bergholtz, J. C. Budich, and F. K. Kunst, Exceptional topology of non-Hermitian systems, Rev. Mod. Phys. **93**, 015005 (2021).

[8] J. Langbehn, Y. Peng, L. Trifunovic, F. von Oppen, and P. W. Brouwer, Reflection-Symmetric Second-Order Topological Insulators and Superconductors, Phys. Rev. Lett. **119**, 246401 (2017).

[9] F. K. Kunst, G. van Miert, and E. J. Bergholtz, Lattice models with exactly solvable topological hinge and corner states, Phys. Rev. B **97**, 241405(R) (2018).

[10] S. Imhof, C. Berger, F. Bayer, J. Brehm, L. W. Molenkamp, T. Kiessling, F. Schindler, C. H. Lee, M. Greiter, T. Neupert, and R. Thomale, Topolectrical-circuit realization of topological corner modes, Nat. Phys. **14**, 925 (2018).

[11] F. Schindler, A. M. Cook, M. G. Vergniory, Z. J. Wang, S. S. P. Parkin, B. A. Bernevig, and T. Neupert, Higher-order topological insulators, Sci. Adv. **4**, eaat0346 (2018).

[12] M. Ezawa, Magnetic second-order topological insulators and semimetals, Phys. Rev. B **97**, 155305 (2018).

[13] F. Schindler, Z. Wang, M. G. Vergniory, A. M. Cook, A. Murani, S. Sengupta, A. Y. Kasumov, R. Deblock, S. J. I. Drozdov, H. Bouchiat, S. Guron, A. Yazdani, B. A. Bernevig, and T. Neupert, Higher-order topology in bismuth, Nat. Phys. **14**, 918 (2018).

[14] J. Noh, W. A. Benalcazar, S. Huang, M. J. Collins, K. P. Chen, T. L. Hughes, and M. C. Rechtsman, Topological protection of photonic mid-gap defect modes, Nat. Photonics **12**, 408 (2018).

[15] M. Geier, L. Trifunovic, M. Hoskam, and P. W. Brouwer, Second-order topological insulators and superconductors with an order-two crystalline symmetry, Phys. Rev. B **97**, 205135 (2018).

[16] T. Liu, Y.-R. Zhang, Q. Ai, Z. P. Gong, K. Kawabata, M. Ueda, and F. Nori, Second-Order Topological Phases in Non-Hermitian Systems, Phys. Rev. Lett. **122**, 076801 (2019).

[17] R. Chen, C.-Z. Chen, J.-H. Gao, B. Zhou, and D.-H. Xu, Higher-Order Topological Insulators in Quasicrystals, Phys. Rev. Lett. **124**, 036803 (2020).

[18] Y. M. Che, C. Gneiting, T. Liu, and F. Nori, Topological quantum phase transitions retrieved through unsupervised machine learning, Phys. Rev. B **102**, 134213 (2020).

[19] B. Zhu, S. Hu, H. H. Zhong, and Y. G. Ke, Uncovering band topology via quantized drift in two-dimensional Bloch oscillations, Phys. Rev. B **104**, 104314 (2021).

[20] I. Mondragon-Shem, T. L. Hughes, J. T. Song, and E. Prodan, Topological Criticality in the Chiral-Symmetric AIII Class at Strong Disorder, Phys. Rev. Lett. **113**, 046802 (2014).

[21] S. Mittal, J. Fan, S. Faez, A. Migdall, J. M. Taylor, and M. Hafezi, Topologically Robust Transport of Photons in a Synthetic Gauge Field, Phys. Rev. Lett. **113**, 087403 (2014).

[22] E. J. Meier, F. A. An, A. Dauphin, M. Maffei, P. Massignan, T. L. Hughes, and B. Gadway, Observation of the topological Anderson insulator in disordered atomic wires, Science **362**, 929 (2018).

[23] M. A. Bandres, S. Wittek, G. Harari, M. Parto, J. H. Ren, M. Segev, D. N. Christodoulides, and M. Khajavikhan, Topological insulator laser: Experiments, Science **359**, eaar4005 (2018).

[24] P. St-Jean, V. Goblot, E. Galopin, A. Lemaître, T. Ozawa, L. Le Gratiet, I. Sagnes, J. Bloch, and A. Amo, Lasing in topological edge states of a one-dimensional lattice, Nat. Photonics **11**, 651 (2017).

[25] H. Zhao, P. Miao, M. H. Teimourpour, S. Malzard, R. El-Ganainy, H. Schomerus, and L. Feng, Topological hybrid silicon microlasers, Nat. Commun. **9**, 981 (2018).

[26] M. Parto, S. Wittek, H. Hodaei, G. Harari, M. A. Bandres, J. H. Ren, M. C. Rechtsman, M. Segev, D. N. Christodoulides, and

M. Khajavikhan, Edge-Mode Lasing in 1D Topological Active Arrays, Phys. Rev. Lett. **120**, 113901 (2018).

[27] G. Harari, M. A. Bandres, Y. Lumer, M. C. Rechtsman, Y. D. Chong, M. Khajavikhan, D. N. Christodoulides, and M. Segev, Topological insulator laser: Theory, Science **359**, eaar4003 (2018).

[28] Y. Bahri, R. Vosk, E. Altman, and A. Vishwanath, Localization and topology protected quantum coherence at the edge of hot matter, Nat. Commun. **6**, 7341 (2015).

[29] W. Nie, Z. H. Peng, F. Nori, and Y.-X. Liu, Topologically Protected Quantum Coherence in a Superatom, Phys. Rev. Lett. **124**, 023603 (2020).

[30] N. Y. Yao, C. R. Laumann, A. V. Gorshkov, H. Weimer L. Jiang, J. I. Cirac, P. Zoller, and M. D. Lukin, Topologically protected quantum state transfer in a chiral spin liquid, Nat. Commun. **4**, 1585 (2013).

[31] J. K. Asbóth, L. Oroszlány, and A. Pályi, *A Short Course on Topological Insulators* (Springer, New York, 2016).

[32] S. H. Shenker and D. Stanford, Black holes and the butterfly effect, J. High Energy Phys. 03 (2014) 067.

[33] S. H. Shenker and D. Stanford, Stringy effects in scrambling, J. High Energy Phys. 05 (2015) 132.

[34] J. Maldacena, S. H. Shenker, and D. Stanford, A bound on chaos, J. High Energy Phys. 08 (2016) 106.

[35] K. Jensen, Chaos in AdS_2 Holography, Phys. Rev. Lett. **117**, 111601 (2016).

[36] D. A. Roberts and B. Swingle, Lieb-Robinson Bound and the Butterfly Effect in Quantum Field Theories, Phys. Rev. Lett. **117**, 091602 (2016).

[37] A. M. García-García, B. Loureiro, A. Romero-Bermúdez, and M. Tezuka, Chaotic-Integrable Transition in the Sachdev-Ye-Kitaev Model, Phys. Rev. Lett. **120**, 241603 (2018).

[38] B. Swingle, Unscrambling the physics of out-of-time-order correlators, Nat. Phys. **14**, 988 (2018).

[39] R. J. Glauber, The quantum theory of optical coherence, Phys. Rev. **130**, 2529 (1963).

[40] M. O. Scully and M. Suhail Zubairy, *Quantum Optics* (Cambridge University Press, Cambridge, 1997).

[41] G. Agarwal, *Quantum Optics* (Cambridge University Press, Cambridge, 2013).

[42] W. Salmon, C. Gustin, A. Settineri, O. Di Stefano, D. Zueco, S. Savasta, F. Nori, and S. Hughes, Gauge-independent emission spectra and quantum correlations in the ultrastrong coupling regime of open system cavity-QED, Nanophotonics **11**, 1573 (2022).

[43] A. Mercurio, V. Macrì, C. Gustin, S. Hughes, S. Savasta, and F. Nori, Regimes of cavity QED under incoherent excitation: From weak to deep strong coupling, Phys. Rev. Res. **4**, 023048 (2022).

[44] D. A. Roberts and D. Stanford, Diagnosing Chaos Using Four-Point Functions in Two-Dimensional Conformal Field Theory, Phys. Rev. Lett. **115**, 131603 (2015).

[45] Y. F. Gu and X.-L. Qi, Fractional statistics and the butterfly effect, J. High Energy Phys. 08 (2016) 129.

[46] G. Zhu, M. Hafezi, and T. Grover, Measurement of many-body chaos using a quantum clock, Phys. Rev. A **94**, 062329 (2016).

[47] I. L. Aleiner, L. Faoro, and L. B. Ioffe, Microscopic model of quantum butterfly effect: Out-of-time-order correlators and traveling combustion waves, Ann. Phys. (Amsterdam) **375**, 378 (2016).

[48] E. B. Rozenbaum, S. Ganeshan, and V. Galitski, Lyapunov Exponent and Out-of-Time-Ordered Correlator's Growth Rate in a Chaotic System, Phys. Rev. Lett. **118**, 086801 (2017).

[49] I. García-Mata, M. Saraceno, R. A. Jalabert, A. J. Roncaglia, and D. A. Wisniacki, Chaos Signatures in the Short and Long Time Behavior of the Out-of-Time Ordered Correlator, Phys. Rev. Lett. **121**, 210601 (2018).

[50] A. Nahum, S. Vijay, and J. Haah, Operator Spreading in Random Unitary Circuits, Phys. Rev. X **8**, 021014 (2018).

[51] C.-J. Lin and O. I. Motrunich, Out-of-time-ordered correlators in a quantum Ising chain, Phys. Rev. B **97**, 144304 (2018).

[52] S. V. Syzranov, A. V. Gorshkov, and V. Galitski, Out-of-time-order correlators in finite open systems, Phys. Rev. B **97**, 161114(R) (2018).

[53] C. W. von Keyserlingk, T. Rakovszky, F. Pollmann, and S. Sondhi, Operator Hydrodynamics, OTOCs, and Entanglement Growth in Systems without Conservation Laws, Phys. Rev. X **8**, 021013 (2018).

[54] V. Khemani, A. Vishwanath, and D. A. Huse, Operator Spreading and the Emergence of Dissipative Hydrodynamics under Unitary Evolution with Conservation Laws, Phys. Rev. X **8**, 031057 (2018).

[55] A. Chan, A. De Luca, and J. T. Chalker, Solution of a Minimal Model for Many-Body Quantum Chaos, Phys. Rev. X **8**, 041019 (2018).

[56] Y. X. Liao and V. Galitski, Nonlinear sigma model approach to many-body quantum chaos: Regularized and unregularized out-of-time-ordered correlators, Phys. Rev. B **98**, 205124 (2018).

[57] E. B. Rozenbaum, S. Ganeshan, and V. Galitski, Universal level statistics of the out-of-time-ordered operator, Phys. Rev. B **100**, 035112 (2019).

[58] T. R. Xu, T. Scaffidi, and X. Y. Cao, Does Scrambling Equal Chaos? Phys. Rev. Lett. **124**, 140602 (2020).

[59] Y. Cao, Y.-N. Zhou, T.-T. Shi, and W. Zhang, Towards quantum simulation of Sachdev-Ye-Kitaev model, Sci. Bull. **65**, 1170 (2020).

[60] T. Akutagawa, K. Hashimoto, T. Sasaki, and R. Watanabe, Out-of-time-order correlator in coupled harmonic oscillators, J. High Energy Phys. 08 (2020) 013.

[61] J. R. G. Alonso, N. Shammah, S. Ahmed, F. Nori, and J. Dressel, Diagnosing quantum chaos with out-of time-ordered-correlator quasiprobability in the kicked-top model, arXiv:2201.08175.

[62] P. D. Blocher, S. Asaad, V. Mourik, M. A. I. Johnson, A. Morello, and K. Mølmer, Measuring out-of-time-ordered correlation functions without reversing time evolution, Phys. Rev. A **106**, 042429 (2022).

[63] R.-Q. He and Z.-Y. Lu, Characterizing many-body localization by out-of-time-ordered correlation, Phys. Rev. B **95**, 054201 (2017).

[64] B. Swingle and D. Chowdhury, Slow scrambling in disordered quantum systems, Phys. Rev. B **95**, 060201(R) (2017).

[65] R. H. Fan, P. F. Zhang, H. T. Shen, and H. Zhai, Out-of-time-order correlation for many-body localization, Sci. Bull. **62**, 707 (2017).

[66] Y. Huang, Y. Zhang, and X. Chen, Out-of-time-ordered correlators in many-body localized systems, Ann. Phys. (Berlin) **529**, 1600318 (2017).

[67] X. Chen, T. C. Zhou, D. A. Huse, and E. Fradkin, Out-of-time-order correlations in many-body localized and thermal phases, Ann. Phys. (Berlin) **529**, 1600332 (2017).
[68] Y. F. Gu, A new tool for quantum chaos could be powerful for other problems: an inspiring application to many-body localization, Sci. Bull. **62**, 669 (2017).
[69] A. Smith, J. Knolle, R. Moessner, and D. L. Kovrizhin, Logarithmic Spreading of Out-of-Time-Ordered Correlators without Many-Body Localization, Phys. Rev. Lett. **123**, 086602 (2019).
[70] J. Lee, D. Kim, and D.-H. Kim, Typical growth behavior of the out-of-time-ordered commutator in many-body localized systems, Phys. Rev. B **99**, 184202 (2019).
[71] P. Hosur, X.-L. Qi, D. A. Roberts, and B. Yoshida, Chaos in quantum channels, J. High Energy Phys. 02 (2016) 004.
[72] D. J. Luitz and Y. B. Lev, Information propagation in isolated quantum systems, Phys. Rev. B **96**, 020406(R) (2017).
[73] M. Gärttner, P. Hauke, and A. M. Rey, Relating Out-of-Time-Order Correlations to Entanglement via Multiple-Quantum Coherences, Phys. Rev. Lett. **120**, 040402 (2018).
[74] M. McGinley, A. Nunnenkamp, and J. Knolle, Slow Growth of Out-of-Time-Order Correlators and Entanglement Entropy in Integrable Disordered Systems, Phys. Rev. Lett. **122**, 020603 (2019).
[75] J. Riddell and E. S. Sørensen, Out-of-time ordered correlators and entanglement growth in the random-field XX spin chain, Phys. Rev. B **99**, 054205 (2019).
[76] H. T. Shen, P. F. Zhang, R. H. Fan, and H. Zhai, Out-of-time-order correlation at a quantum phase transition, Phys. Rev. B **96**, 054503 (2017).
[77] M. Heyl, F. Pollmann, and B. Dóra, Detecting Equilibrium and Dynamical Quantum Phase Transitions in Ising Chains via Out-of-Time-Ordered Correlators, Phys. Rev. Lett. **121**, 016801 (2018).
[78] C. B. Dağ, K. Sun, and L.-M. Duan, Detection of Quantum Phases via Out-of-Time-Order Correlators, Phys. Rev. Lett. **123**, 140602 (2019).
[79] Q. Wang and F. Pérez-Bernal, Probing an excited-state quantum phase transition in a quantum many-body system via an out-of-time-order correlator, Phys. Rev. A **100**, 062113 (2019).
[80] B. Chen, X. F. Hou, F. F. Zhou, P. Qian, H. Shen, and N. Y. Xu, Detecting the out-of-time-order correlations of dynamical quantum phase transitions in a solid-state quantum simulator, Appl. Phys. Lett. **116**, 194002 (2020).
[81] Z.-H. Sun, J.-Q. Cai, Q.-C. Tang, Y. Hu, and H. Fan, Out-of-time-order correlators and quantum phase transitions in the Rabi and Dicke models, Ann. Phys. (Berlin) **532**, 1900270 (2020).
[82] R. J. Lewis-Swan, S. R. Muleady, and A. M. Rey, Detecting Out-of-Time-Order Correlations via Quasiadiabatic Echoes as a Tool to Reveal Quantum Coherence in Equilibrium Quantum Phase Transitions, Phys. Rev. Lett. **125**, 240605 (2020).
[83] M. Gärttner, J. G. Bohnet, A. Safavi-Naini, M. L. Wall, J. J. Bollinger, and A. M. Rey, Measuring out-of-time-order correlations and multiple quantum spectra in a trapped-ion quantum magnet, Nat. Phys. **13**, 781 (2017).
[84] J. Li, R. H. Fan, H. Y. Wang, B. T. Ye, B. Zeng, H. Zhai, X. H. Peng, and J. F. Du, Measuring Out-of-Time-Order Correlators on a Nuclear Magnetic Resonance Quantum Simulator, Phys. Rev. X **7**, 031011 (2017).
[85] K. X. Wei, P. Peng, O. Shtanko, I. Marvian, S. Lloyd, C. Ramanathan, and P. Cappellaro, Emergent Prethermalization Signatures in Out-of-Time Ordered Correlations, Phys. Rev. Lett. **123**, 090605 (2019).
[86] X. F. Nie, B.-B. Wei, X. Chen, Z. Zhang, X. Z. Zhao, C. D. Qiu, Y. Tian, Y. L. Ji, T. Xin, D. W. Lu, and J. Li, Experimental Observation of Equilibrium and Dynamical Quantum Phase Transitions via Out-of-Time-Ordered Correlators, Phys. Rev. Lett. **124**, 250601 (2020).
[87] K. A. Landsman, C. Figgatt, T. Schuster, N. M. Linke, B. Yoshida, N. Y. Yao, and C. Monroe, Verified quantum information scrambling, Nature (London) **567**, 61 (2019).
[88] E. L. Hahn, Spin echoes, Phys. Rev. **80**, 580 (1950).
[89] B. Swingle, G. Bentsen, M. Schleier-Smith, and P. Hayden, Measuring the scrambling of quantum information, Phys. Rev. A **94**, 040302(R) (2016).
[90] C. M. Sánchez, A. K. Chattah, K. X. Wei, L. Buljubasich, P. Cappellaro, and H. M. astawski, Perturbation Independent Decay of the Loschmidt Echo in a Many-Body System, Phys. Rev. Lett. **124**, 030601 (2020).
[91] W. P. Su, J. R. Schrieffer, and A. J. Heeger, Solitons in Polyacetylene, Phys. Rev. Lett. **42**, 1698 (1979).
[92] S. Rufo, N. Lopes, M. A. Continentino, and M. A. R. Griffith, Multicritical behavior in topological phase transitions, Phys. Rev. B **100**, 195432 (2019).
[93] M. Creutz, End States, Ladder Compounds, and Domain-Wall Fermions, Phys. Rev. Lett. **83**, 2636 (1999).
[94] See Supplemental Material at http://link.aps.org/supplemental/10.1103/PhysRevB.107.L020202 for the detailed derivation of the analytical OTOC dynamics for the nearest-neighbor SSH model, discussion of the OTOC witness when the initial state is the eigenstate of the system, additional discussion of the application of the OTOC witness in disordered systems, discussion of the application of the OTOC witness in a two-dimensional lattice described by the Qi-Wu-Zhang model, and discussion of the application of the OTOC witness in non-Hermitian systems, which includes Refs. [95–105].
[95] B. C. Shin, A formula for eigenpairs of certain symmetric tridiagonal matrices, Bull. Aust. Math. Soc. **55**, 249 (1997).
[96] X.-L. Qi, Y.-S. Wu, and S.-C. Zhang, Topological quantization of the spin Hall effect in two-dimensional paramagnetic semiconductors, Phys. Rev. B **74**, 085308 (2006).
[97] D. Leykam, K. Y. Bliokh, C. Huang, Y. D. Chong, and F. Nori, Edge Modes, Degeneracies, and Topological Numbers in Non-Hermitian Systems, Phys. Rev. Lett. **118**, 040401 (2017).
[98] C. Gneiting, A. Koottandavida, A. V. Rozhkov, and F. Nori, Unraveling the topology of dissipative quantum systems, Phys. Rev. Res. **4**, 023036 (2022).
[99] F. Minganti, I. I. Arkhipov, A. Miranowicz, and F. Nori, Continuous dissipative phase transitions with or without symmetry breaking, New J. Phys. **23**, 122001 (2021).
[100] C. Leefmans, A. Dutt, J. Williams, L. Q. Yuan, M. Parto, F. Nori, S. Fan, and A. Marandi, Topological dissipation in a time-multiplexed photonic resonator network, Nat. Phys. **18**, 442 (2022).
[101] S. Lieu, Topological phases in the non-Hermitian Su-Schrieffer-Heeger model, Phys. Rev. B **97**, 045106 (2018).
[102] F. K. Kunst, E. Edvardsson, J. C. Budich, and E. J. Bergholtz, Biorthogonal Bulk-Boundary Correspondence in Non-Hermitian Systems, Phys. Rev. Lett. **121**, 026808 (2018).

[103] S. Y. Yao and Z. Wang, Edge States and Topological Invariants of Non-Hermitian Systems, Phys. Rev. Lett. **121**, 086803 (2018).
[104] C. H. Yin, H. Jiang, L. H. Li, R. Lü, and S. Chen, Geometrical meaning of winding number and its characterization of topological phases in one-dimensional chiral non-Hermitian systems, Phys. Rev. A **97**, 052115 (2018).
[105] L. Jin and Z. Song, Symmetry-protected scattering in non-Hermitian linear systems, Chin. Phys. Lett. **38**, 024202 (2021).
[106] F. D. M. Haldane, Model for a Quantum Hall Effect without Landau Levels: Condensed-Matter Realization of the "Parity Anomaly", Phys. Rev. Lett. **61**, 2015 (1988).
[107] G. Jotzu, M. Messer, R. Desbuquois, M. Lebrat, T. Uehlinger, D. Greif, and T. Esslinger, Experimental realization of the topological Haldane model with ultracold fermions, Nature (London) **515**, 237 (2014).
[108] W. A. Benalcazar, B. A. Bernevig, and T. L. Hughes, Quantized electric multipole insulators, Science **357**, 61 (2017).
[109] C. W. Peterson, W. A. Benalcazar, T. L. Hughes, and G. Bahl, A quantized microwave quadrupole insulator with topologically protected corner states, Nature (London) **555**, 346 (2018).
[110] M. Serra-Garcia, V. Peri, R. Süsstrunk, O. R. Bilal, T. Larsen, L. G. Villanueva, and S. D. Huber, Observation of a phononic quadrupole topological insulator, Nature (London) **555**, 342 (2018).
[111] S. Mittal, V. V. Orre, G. Zhu, M. A. Gorlach, A. Poddubny, and M. Hafezi, Photonic quadrupole topological phases, Nat. Photonics **13**, 692 (2019).
[112] P. Nevado, S. Fernández-Lorenzo, and D. Porras, Topological Edge States in Periodically Driven Trapped-Ion Chains, Phys. Rev. Lett. **119**, 210401 (2017).
[113] H. Häffner, C. F. Roos, and R. Blatt, Quantum computing with trapped ions, Phys. Rep. **469**, 155 (2008).
[114] R. Blatt and C. F. Roos, Quantum simulations with trapped ions, Nat. Phys. **8**, 277 (2012).
[115] C. Monroe, W. C. Campbell, L.-M Duan, Z.-X Gong, A. V. Gorshkov, P. W. Hess, R. Islam, K. Kim, N. M. Linke, G. Pagano, P. Richerme, C. Senko, and N. Y. Yao, Programmable quantum simulations of spin systems with trapped ions, Rev. Mod. Phys. **93**, 025001 (2021).
[116] W. Cai, J. Han, F. Mei, Y. Xu, Y. Ma, X. Li, H. Wang, Y. P. Song, Z.-Y. Xue, Z.-q. Yin, S. Jia, and L. Sun, Observation of Topological Magnon Insulator States in a Superconducting Circuit, Phys. Rev. Lett. **123**, 080501 (2019).
[117] T. H. Wang, Z. X. Zhang, L. Xiang, Z. H. Gong, J. L. Wu, and Y. Yin, Simulating a topological transition in a superconducting phase qubit by fast adiabatic trajectories, Sci. China: Phys. Mech. Astron. **61**, 047411 (2018).
[118] S. K. Zhao, Z.-Y. Ge, Z. C. Xiang, G. M. Xue, H. S. Yan, Z. T. Wang, Z. Wang, H. K. Xu, F. F. Su, Z. H. Yang, H. Zhang, Y.-R. Zhang, X.-Y. Guo, K. Xu, Y. Tian, H. F. Yu, D. N. Zheng, H. Fan, and S. P. Zhao, Probing Operator Spreading via Floquet Engineering in a Superconducting Circuit, Phys. Rev. Lett. **129**, 160602 (2022).
[119] M. Atala, M. Aidelsburger, J. T. Barreiro, D. Abanin, T. Kitagawa, E. Demler, and I. Bloch, Direct measurement of the Zak phase in topological Bloch bands, Nat. Phys. **9**, 795 (2013).
[120] S. de Léséleuc, V. Lienhard, P. Scholl, D. Barredo, S. Weber, N. Lang, H. P. Büchler, T. Lahaye, and A. Browaeys, Observation of a symmetry-protected topological phase of interacting bosons with Rydberg atoms, Science **365**, 775 (2019).
[121] M. Lohse, C. Schweizer, O. Zilberberg, M. Aidelsburger, and I. Bloch, A Thouless quantum pump with ultracold bosonic atoms in an optical superlattice, Nat. Phys. **12**, 350 (2016).